An Eight-Device Extended-Resonance Power-Combining Amplifier

Adam L. Martin, Amir Mortazawi, *Member, IEEE*, and Bernard C. DeLoach, Jr., *Life Fellow, IEEE*

***Abstract*— An extended resonance technique for designing power amplifiers is investigated. This technique provides a planar power-combining structure whose primary distinction from conventional structures is that it does not require quarter-wave or multiple quarter-wave spacing between devices. A theoretical analysis of extended-resonance combiners is presented, followed by experimental data from an eight-device power amplifier. This approach is adaptable to monolithic circuit-fabrication techniques and should be useful for millimeter-wave applications.**

I. Introduction

THE greatest need for power combining is at microwave and millimeter-wave frequencies where an individual solid-state device is often incapable of producing adequate power for most radar and communication systems. To remedy this, power combiners are used to obtain sufficient power from solid-state devices. Typical power combiners employ Wilkinson or hybrid structures in which devices are interconnected with quarter-wave transmission lines to achieve power combining [1]–[7]. These structures become quite large when many devices are employed. Such large combining structures often have losses that rival the device gains, limiting their use at high frequencies.

An extended-resonance technique was introduced and applied to power-combining oscillators in [8]. A four-device power-combining amplifier based on extended resonance was later presented in [9]. Extended resonance effectively places devices in shunt to combine the power from each device. The magnitude of the voltage at each device is the same, and the gain of the extended-resonance amplifier is equal to the gain of a single-device amplifier. The significance of extended resonance lies in its ability to either divide power between, or combine power from, devices without the need for quarter-wave or half-wave transmission lines. Shorter line lengths may be used. This enables a compact circuit to be designed that is particularly suitable for monolithic microwave integrated circuit (MMIC) implementation. This method may also be used in conjunction with conventional methods to enhance their performance.

In this paper, a comprehensive study of extended-resonance power-combining amplifiers is discussed. This study develops the theoretical power-combining mechanism of extended resonance along with experimental results from a new eight-device power amplifier at X-band. This eight-device amplifier handles twice as much power as the four-device amplifier presented in [9]. In addition, the eight-device amplifier presented here utilizes shorter transmission lines and maintains the same bandwidth achieved with the four-device amplifier.

The extended-resonance amplifier is superficially similar in structure to a distributed amplifier [3], but is actually quite different in its performance. The distributed amplifier is a traveling-wave structure, while the extended-resonance amplifier is actually a power-combining circuit; each device amplifying the same magnitude excitation. In addition, the gain of the extended-resonance multiple-device amplifier is the same as that for a single-device amplifier (assuming lossless transmission lines) regardless of the number of devices used in the circuit. This is indeed not the case for distributed amplifiers.

The authors have recently become aware of previous work on "ladder-type" microwave power-divider/combiner structures in rectangular waveguides [10], [11] that is somewhat similar to work reported herein. In [10] and [11], separate three-port passive power-divider and power-combiner systems in rectangular waveguide were implemented. However, when designing power amplifiers based on this technique, certain constraints are placed on the design of the dividing and combining circuits. A design technique that addresses these constraints is presented in this paper. Furthermore, an eight-device extended-resonance amplifier is constructed using microstrip.

II. Extended-Resonance Power-Combining Amplifiers

Fig. 1 illustrates one version of an extended-resonance power-combining amplifier utilizing n-FET's. Both the gates and drains are sequentially linked with transmission lines. The electrical lengths of the transmission lines connecting each device are denoted by θg_m and θd_m for the gate lines and the drain lines, respectively, where $1 \leq m \leq n-1$. The input and output are located at the gate of the first device and the drain of the nth device, respectively. It is assumed that each device has the same gate admittance $Yg = Gg + jBg$ and drain admittance $Yd = Gd + jBd$. The dividing and combining circuits may be considered separately, as shown in Figs. 2 and 3. Here, the gate and drain admittances may be assumed to be the simultaneous conjugate match admittances. In Fig. 2, line length θg_{n-1} transforms $Y = Gg + jBg$ from the nth device, to its conjugate $Y^* = Gg - jBg$ at the location of the next device. Adding the gate admittance of

Manuscript received November 11, 1996; revised March 9, 1998. The work of A. L. Martin was supported by a grant from the Florida Space Grant Consortium.

The authors are with the Department of Electrical and Computer Engineering, University of Central Florida, Orlando, FL 32816 USA.

Publisher Item Identifier S 0018-9480(98)04050-2.

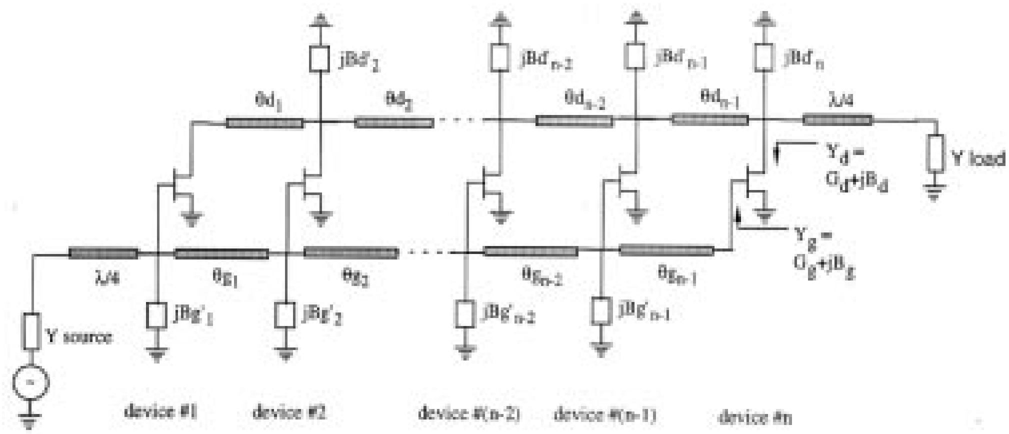

Fig. 1. An n-device extended-resonance amplifier.

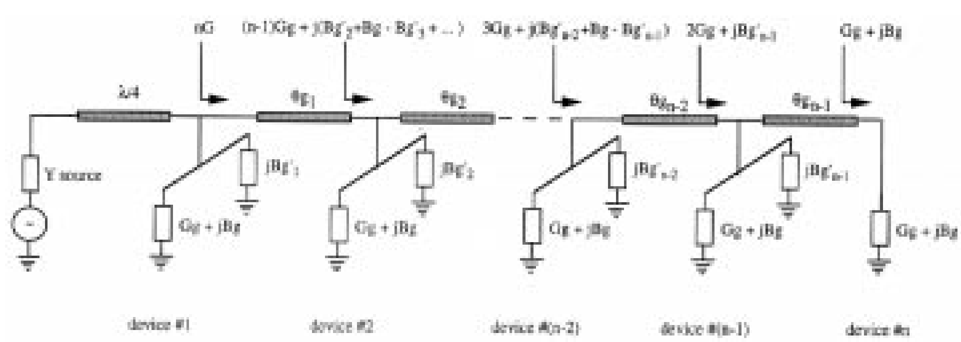

Fig. 2. Input circuit.

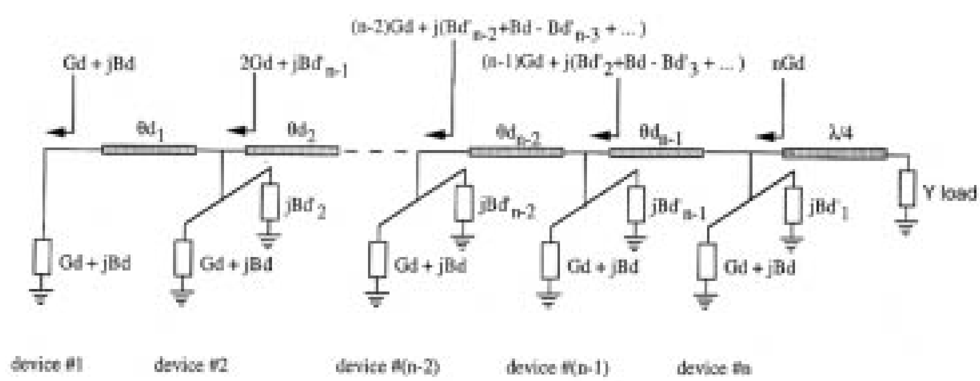

Fig. 3. Output circuit.

the next device, the imaginary components cancel; hence, the gate admittance at device $n-1$ is $2G_g$. A shunt susceptive element, jBg'_{n-1} may be placed at this device so that line length θg_{n-2} transforms $Y = 2G_g + jBg'n-1$ from the second device to its conjugate $Y^* = 2G_g - jBg'_{n-1}$ at the next device (the choice of jBg'_{n-1} is, at this point, completely arbitrary). This process continues all the way to the gate of the first device. The shunt susceptance, jBg'_1 can be chosen to cancel the total reactive component at the input, and the input admittance nGg can be matched to a given source admittance using a quarter-wave transformer. Similarly, in the drain circuit of Fig. 3, length θd_1 transforms $Y = Gd + jBd$ from the first device to $Y^* = Gd - jBd$ at the second device. Line length θd_2 transforms $Y = 2Gd + jBd'_{n-1}$ at the second device to $Y = 2Gd - jBd'_2$ at the third device. This continues to the drain of the nth device, where the leftover susceptance is canceled by jBd'_n.

The basic design procedure for an extended-resonance power amplifier will now be considered. It will be shown that an input signal applied to the gate of the first FET will be divided equally among all FET's. Each FET amplifies 1/n of the input power and delivers it to the output combining circuit where the power from each FET is recombined at the load. Assuming lossless lines, it can also be shown that the total output power is equal to n times the power generated by each device.

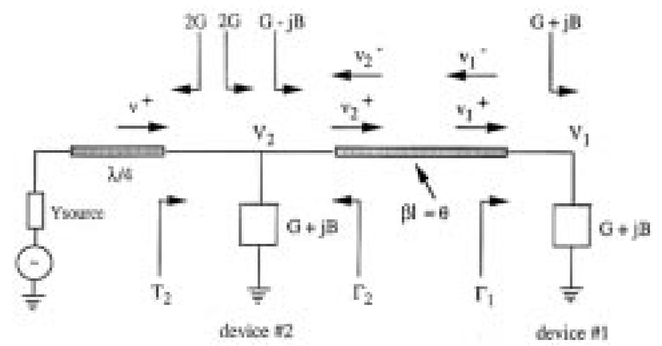

Fig. 4. Analysis of input circuit.

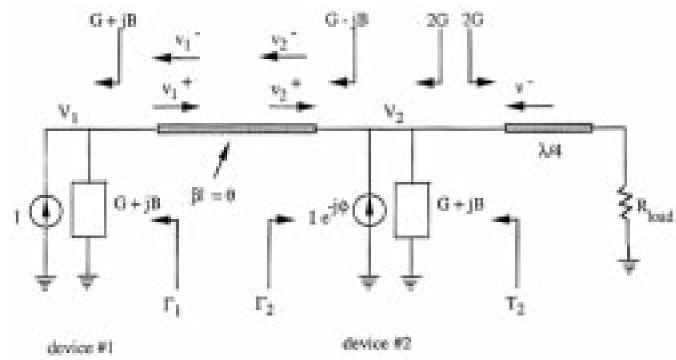

Fig. 5. Analysis of output circuit.

III. Analysis of the Gate Extended-Resonance Circuit

For simplicity, consider the two-device extended-resonance circuit shown in Fig. 4. Two devices, each represented by a normalized admittance $G + jB$, are connected with a transmission line of electrical length θ and characteristic admittance Y_o. An analysis of this circuit can be done by determining the forward and reverse steady-state traveling waves along the transmission line after a source is applied to the input. Referring to Fig. 4, Γ_1 is the reflection coefficient looking to the right at the first device, Γ_2 is the reflection coefficient looking to the left at the second device, and T_2 is the transmission coefficient looking to the right at the second device. Γ_1, Γ_2, and T_2 can be expressed in terms of Y_o, G, and B as

$$\Gamma_1 = \frac{Y_o - G - jB}{Y_o + G + jB} \tag{1}$$

$$\Gamma_2 = \frac{Y_o - 3G - jB}{Y_o + 3G + jB} \tag{2}$$

$$T_2 = \frac{2Y}{Y_o + 2G}. \tag{3}$$

In the following equations, it will be convenient to express Γ_1 in terms of its magnitude and phase angle γ:

$$\Gamma_1 = |\Gamma_1| e^{j\gamma}$$

The voltage V_1 across the terminals of the first device is expressed in terms of the forward and reverse traveling waves at port 1:

$$V_1 = v_1^- + v_1^+. \tag{4}$$

Similarly, for V_2,

$$V_2 = v_2^- + v_2^+. \tag{5}$$

V_1 and V_2 can be rewritten as

$$V_1 = \frac{T_2[1 + \Gamma_1]e^{-j\theta}}{1 - \Gamma_1\Gamma_2 e^{-j2\theta}} v^+ \tag{6}$$

$$V_2 = \frac{T_2[1 + \Gamma_1 e^{-j2\theta}]}{1 - \Gamma_1\Gamma_2 e^{-j2\theta}} v^+ \tag{7}$$

where v^+ is the incident wave at the input (see Fig. 4). From (6) and (7), the ratio of V_1 and V_2 is

$$\frac{V_1}{V_2} = \frac{[1 + \Gamma_1]e^{-j\theta}}{1 + \Gamma_1 e^{-j2\theta}}. \tag{8}$$

The length of (lossless) transmission line θ required to transform $Y = G + jB$ to its conjugate $Y^* = G - jB$ can be expressed in terms of the angle γ of the reflection coefficient associated with the admittance $G + jB$ as

$$\theta = \gamma, \qquad \text{when } B < 0$$
$$\theta = \gamma + \pi, \qquad \text{when } B > 0.$$

When $B < 0$, (8) becomes

$$\frac{V_1}{V_2} = \frac{[1 + |\Gamma_1| e^{j\gamma}]e^{-j\gamma}}{1 + |\Gamma_1| e^{-j\gamma}}. \tag{9}$$

The magnitude of the voltage at each device is equal $(|V_1|/|V_2| = 1)$ and V_1 lags V_2 by ϕ where

$$\phi = \gamma - 2\tan^{-1}\left[\frac{|\Gamma_1|\sin\gamma}{1 + |\Gamma_1|\cos\gamma}\right]. \tag{10}$$

When $B > 0$, (8) becomes

$$\frac{V_1}{V_2} = \frac{[1 + |\Gamma_1| e^{j\gamma}]e^{-j(\gamma+\pi)}}{1 + |\Gamma_1| e^{-j\gamma}}. \tag{11}$$

Here again, the magnitude of the voltage at each device is the same, and now V_1 lags V_2 by

$$\phi = \pi + \gamma - 2\tan^{-1}\left[\frac{|\Gamma_1|\sin\gamma}{1 + |\Gamma_1|\cos\gamma}\right]. \tag{12}$$

Equations (10) and (12) are useful for determining the phase shift between devices in a two-device extended-resonance power-dividing circuit. Determining the phase angle ϕ only requires knowledge of the transmission line length θ and the reflection coefficient (Γ_1) at the location of the first device. For an extended-resonance circuit containing n devices, the phase shift ϕ between any two devices can be calculated by simply knowing the line lengths and the total reflection coefficient at each device port. For example, to determine the phase shift ϕ between device m and device $m+1$ in an extended-resonance circuit having an arbitrary number of devices, simply substitute Γ_m and θ_m into the above equations for Γ_1 and θ, respectively, where Γ_m is the total reflection coefficient at device m, and θ_m is the electrical length of the transmission line connecting device m to device $m+1$.

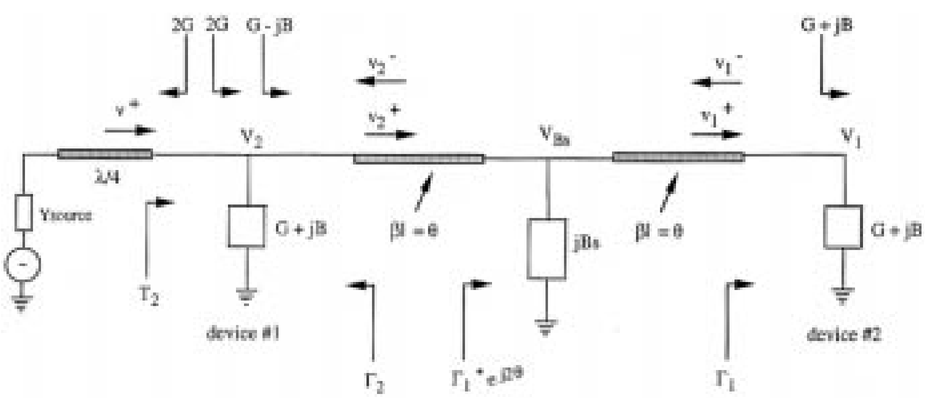

Fig. 6. Analysis of the modified input circuit.

IV. Analysis of the Drain Extended-Resonance Circuit

Consider now the power combiner circuit in Fig. 5, which represents the drain circuit of the power amplifier. The drain of each FET is modeled as a current source and its output admittance. Based on the power-divider analysis for the gate circuit, the current sources have equal magnitudes, with a phase difference ϕ imposed by the gate circuit divider. Once again, (1) and (2) are used to express V_1 and V_2, as shown in (13) and (14), at the bottom of the page. The electrical length θ is once again chosen to be the length of line required to transform $G+jB$ to $G-jB$. It can, therefore, be expressed in terms of the reflection angle γ as was done in the power-dividing scheme. After some mathematical manipulations, the ratio of V_1 to V_2 can be expressed as

$$\frac{V_1}{V_2} = \cos\phi + j\frac{G}{Y_o}\sin\theta. \tag{15}$$

Requiring the condition

$$\frac{G}{Y_o}\sin\theta = \sin\phi \tag{16}$$

to be satisfied by (15) results in V_1 and V_2 having equal magnitudes with a phase difference ϕ. Satisfying (16) results in equal voltage at each device terminal and, consequently, total power being sent to the load.

V. Design Considerations

An extended-resonance amplifier is designed using (10), (12), and (16). The value of ϕ, which is calculated from the gate circuit equation (10) or (12), must be inserted into the drain circuit equation (16) so that one must solve for the transmission-line length Θ in the drain circuit. The length θ must satisfy extended-resonance conditions (θ equals either γ or $\gamma+\pi$, depending on the sign of jB at the drain of the device). Assuming a preset value for both G and Y_o in (16), one must, therefore, determine what value of jB (i.e., the value of the shunt reactive element) at the drain of each device must be in order to produce a length θ that will satisfy (16).

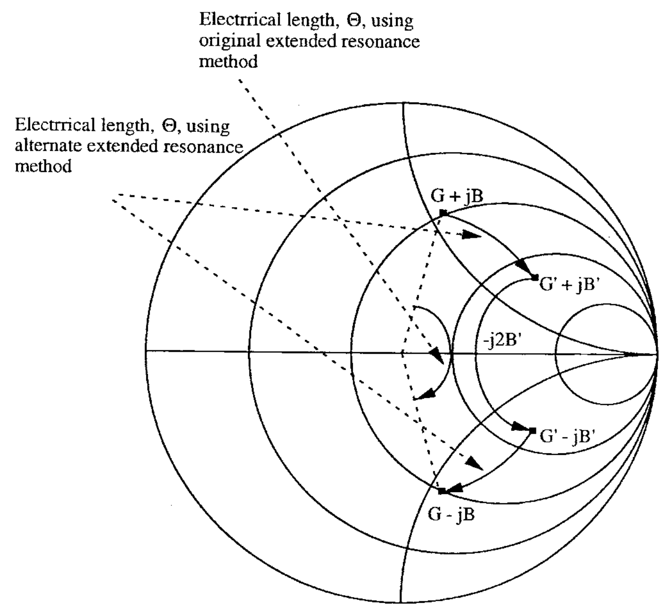

Fig. 7. Smith-chart representation of extended resonance.

Transmission lines in the input circuit may sometimes differ substantially in length from those in the output circuit. It may be necessary to use a modified version of the extended-resonance procedure. For example, consider the simple power-dividing circuit in Fig. 6. The difference between this circuit and that in Fig. 4 is that a shunt reactive element is inserted halfway between the devices. The design procedure for this circuit may be seen on the Smith chart in Fig. 7. Instead of converting the admittance, $Y = G + jB$ of the first

$$V_1 = \frac{\dfrac{I}{Y_o+G+jB}[1+\Gamma_2 e^{-j2\theta}] + \dfrac{Ie^{-j\phi}}{Y_o+3G+jB}[1+\Gamma_1]e^{-j\theta}}{1-\Gamma_1\Gamma_2 e^{-j2\theta}} \tag{13}$$

$$V_2 = \frac{\dfrac{Ie^{-j\phi}}{Y_o+3G+jB}[1+\Gamma_1 e^{-j2\theta}] + \dfrac{I}{Y_o+G+jB}[1+\Gamma_2]e^{-j\theta}}{1-\Gamma_1\Gamma_2 e^{-j2\theta}} \tag{14}$$

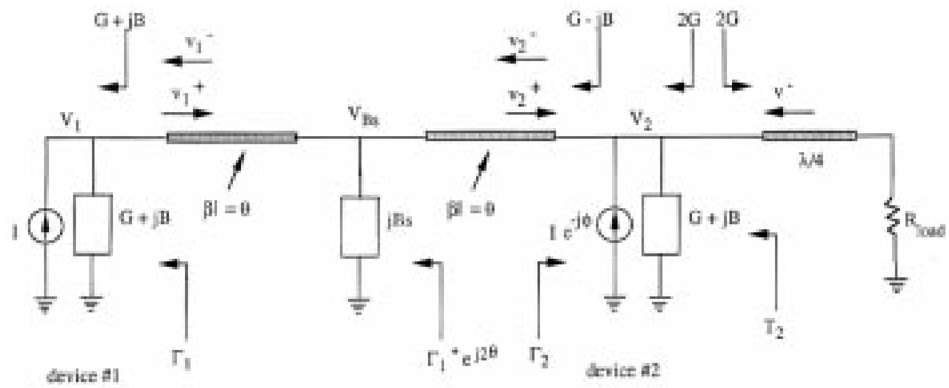

Fig. 8. Analysis of the modified output circuit.

device to its conjugate value $Y^* = G - jB$, the admittance of the first device is transformed to some arbitrary value $Y' = G' + jB'$, where B' may be either positive or negative. This transformation is done by the first half of the transmission line. The shunt susceptance jB's convert $Y' = G' + jB'$ to $Y'^* = G' - jB'$. The second half of the transmission line finally takes $Y'^* = G' - jB'$ to $Y^* = G - jB$, to resonate the susceptance of the second device. With a sinusoidal source at the input, the ratio of the voltage at the first device to the voltage at the second device can be determined from (8) and (9). First, the relationship between the voltage at the first device and the voltage halfway between the two devices (V_x) is found as follows:

$$\frac{V_1}{V_x} = \frac{[1 + |\Gamma_1| e^{j\gamma}] e^{-j\theta}}{1 + |\Gamma_1| e^{j\gamma} e^{-j2\theta}}. \tag{17}$$

The ratio of V_x to V_2 is

$$\frac{V_x}{V_2} = \frac{[1 + |\Gamma_1| e^{j\gamma} e^{j2\theta}] e^{-j\theta}}{1 + |\Gamma_1| e^{-j\gamma}}. \tag{18}$$

Thus, V_1 is related to V_2 by

$$\frac{V_1}{V_2} = \frac{[1 + |\Gamma_1| e^{-j\gamma} e^{j2\theta}] e^{-j2\theta} [1 + |\Gamma_1| e^{j\gamma}]}{1 + |\Gamma_1| e^{-j\gamma} [1 + |\Gamma_1| e^{j\gamma} e^{-j2\theta}]}. \tag{19}$$

The magnitude of the voltages V_1 and V_2 are the same as before. In this case, V_2 lags V_1 by

$$\phi = 2\theta - 2\tan^{-1}\left[\frac{|\Gamma_1| \sin\gamma}{1 + |\Gamma_1| \cos\gamma}\right] - 2\tan^{-1}\left[\frac{|\Gamma_1| \sin(2\theta - \gamma)}{1 + |\Gamma_1| \cos(2\theta - \gamma)}\right]. \tag{20}$$

Fig. 8 illustrates the power-combining scheme using the alternate method. It can be shown that the relationship between V_1 and V_2 for the power-combining version of this circuit is that of (19) with the phase relationship between V_2 and V_1 reversed.

This implies that instead of placing a susceptive stub at the ends of a transmission line inserted between two devices, a single stub may be placed at the center of a shorter length of transmission line that can be inserted between the same two devices. This allows the designer to vary the physical spacing between devices so that it is approximately the same in both the input and output circuits.

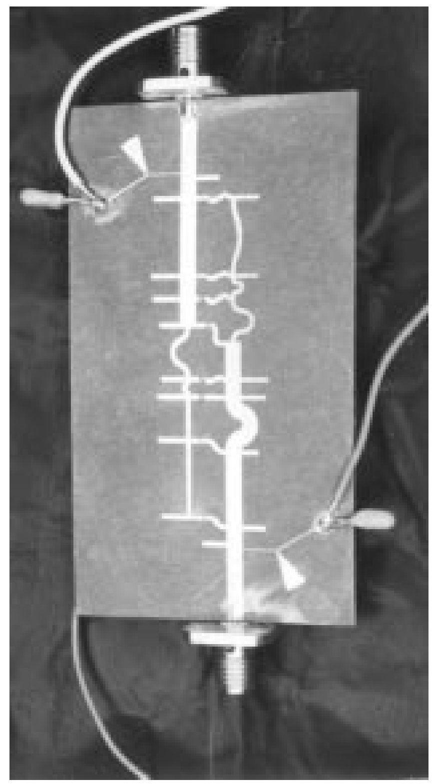

Fig. 9. Photograph of an eight-device extended-resonance amplifier, with the output circuit on top. Circuit measures 73 mm $\times$ 41 mm.

VI. Experiment

An eight-device extended-resonance power-combining amplifier was designed and constructed. An enlarged photograph of the eight-device amplifier is shown in Fig. 9. Circuit-board dimensions are 73 mm $\times$ 41 mm. Microstrip stubs provide the desired susceptance at the terminals of each device. The active devices used were 100-mW alpha-power GaAs MESFET chips AF035p1-00 with a gate length of 0.25 μm and a total gate periphery of 400 μm. Devices were biased at 5 V with a drain current of 70 mA. The amplifier was constructed on a 31-mil-thick Duroid substrate with $\varepsilon_r = 2.33$. The devices were mounted on copper rods with conductive epoxy. The devices were grounded by inserting the rods through holes in the substrate and soldering them to the ground plane. The gate and drain of each device were each connected to the circuit

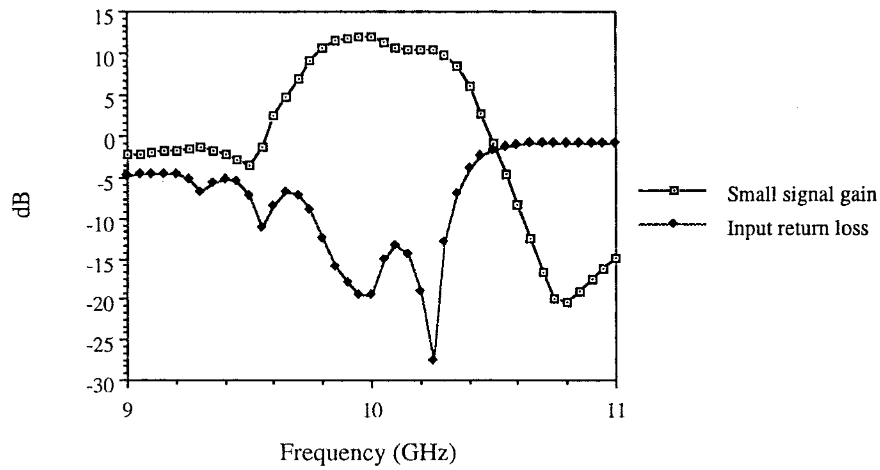

Fig. 10. Predicted small-signal gain and return loss for the eight-device amplifier.

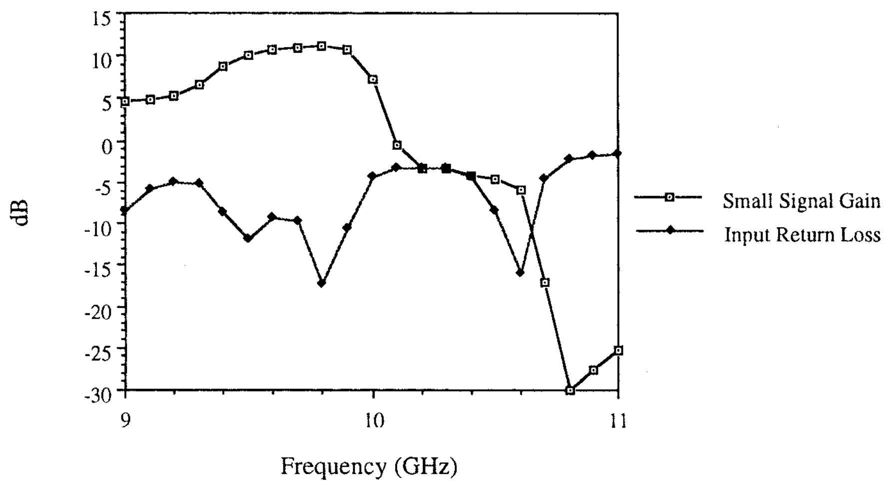

Fig. 11. Measured small-signal gain and return loss for the eight-device amplifier.

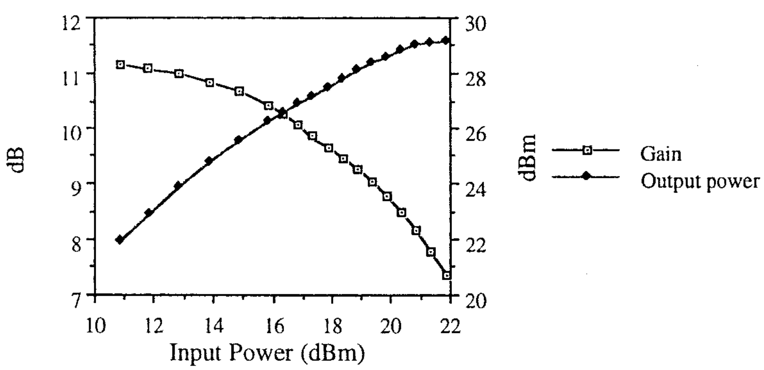

Fig. 12. Measured output power and gain compression curves for the eight-device amplifier.

with bond wire. Fig. 10 shows the predicted small-signal gain and return loss. At 10 GHz, the predicted small-signal gai was 11.9 dB. Fig. 11 shows the measured small-signal gain and return loss. At 9.8 GHz, the measured small-signal gain was 11.2 dB. The predicted and measured performance are very close, except that the measured response is shifted down by about 200 MHz. Otherwise, the measured response is well matched to the predicted performance. The shift in frequency can be due to the inaccuracies in modeling wire bonds and mounting the chips on the substrate. Output power and gain versus input power at 9.8 GHz is plotted in Fig. 12. At 1-dB compression, the output power is 582 mW with a power-added efficiency of 18.29%. At 3-dB compression, the output power is 813 mW with a power-added efficiency of 30.44%. In order to determine the power-combining performance of the eight-device amplifier, a single-device amplifier was also built and tested. The maximum small-signal gain was 11.5 dB at 9.6 GHz. At the 3-dB compression point, the output power was 111 mW with a power-added efficiency of 33.7%. This indicates a power-combining efficiency of 91.6% for the eight-device amplifier. The measured 3-dB bandwidth for each amplifier was approximately 5%. As previously mentioned, this bandwidth should meet the demands of many millimeter-wave systems.

VII. Conclusion

An eight-device amplifier based on an extended-resonance technique has been presented. The amplifier was able to produce approximately eight times the power available from a single-device amplifier. Furthermore, a general extended-resonance amplifier design procedure was outlined such that the voltage phase delay in the dividing and combining circuits can be more easily manipulated to permit a combiner circuit with line lengths that are similar to the lengths used in the divider circuit. This general approach alleviates the problem of matching the voltage phase delay through the input and output circuits of the amplifier. Amplifiers based on this more general extended-resonance approach are currently underway. Anticipated goals include the design of a monolithic extended-resonance power-combining amplifier at millimeter-wave frequencies.

References

[1] K. J. Russell, "Microwave power combining techniques," *IEEE Trans. Microwave Theory Tech.,* vol. MTT-27, pp. 472–478, May 1979.
[2] K. Chang and C. Sun, "Millimeter-wave power combining techniques," *IEEE Trans. Microwave Theory Tech.,* vol. MTT-31, pp. 91–107, Feb. 1983.
[3] G. D. Vendelin, A. M. Pavio, and U. L. Rohde, *Microwave Circuit Design Using Linear and Nonlinear Techniques.* New York: Wiley, 1990.
[4] A. G. Bert and D. Kaminsky, "The travelling wave power divider/combiner," in *IEEE MTT-Symp. Dig.,* Washington, DC, May 1980, pp. 487–489.
[5] N. Camilleri, B. Kim, H. Q. Tserng, and H. D. Shih, "Ka-band monolithic GaAs FET power amplifier modules," in *IEEE MTT-Symp. Dig.,* New York, NY, May 1988, pp. 179–182.
[6] H. Q. Tserng and P. Saunier, "10–30 GHz monolithic GaAs travelling-wave divider/combiner," *Electron. Lett.,* vol. 21, pp. 950–951, 1985.
[7] M. Faulkner, P. Chye, and R. Hansen, "V-band PHEMT power amplifier using an n-way chain combiner," in *IEEE MTT-Symp. Dig.,* vol. 1, San Diego, CA, May 1994, pp. 265–268.
[8] A. Mortazawi and B. C. DeLoach, Jr., "Multiple element oscillators utilizing a new power combining technique," *IEEE Trans. Microwave Theory Tech.,* vol. 40, pp. 2397–2402, Dec. 1992.
[9] A. L. Martin, A. Mortazawi, and B. C. DeLoach, Jr., "A power amplifier based on an extended resonance technique," *IEEE Microwave Guided Wave Lett.,* vol. 5, pp. 329–331, Oct. 1995.
[10] K. Fukui, S. Nogi, A. Sanada, and S. Oishi, "Ladder-type microwave power divider/combiners," *Electron. Commun. Japan,,* vol. 74, pt. 2, no. 8, pp. 25–39, Jan. 1991.
[11] S. Nogi and K. Fukui, "Optimum design and performance of a microwave ladder oscillator with many diode mount pairs," *IEEE Trans. Microwave Theory Tech.,* vol. MTT-30, pp. 735–743, May, 1982.

Adam L. Martin was born March 22, 1971, in Detroit, MI. He has received the B.S.E.E. and M.S.E.E. degrees from the University of Central Florida, Orlando, in 1994 and 1995, respectively, and is currently working toward the Ph.D. degree in the area of microwave active circuit design.

Mr. Martin is a member of Eta Kappa Nu.

Amir Mortazawi (S'87–M'90) was born in Iran, in 1962. He received the B.S. degree in electrical engineering from the State University of New York at Stony Brook, in 1987, and the M.S. and Ph.D. degrees in electrical engineering from the University of Texas at Austin, in 1988 and 1990, respectively.

In 1990, he joined the University of Central Florida, Orlando, where he is currently an Associate Professor of electrical engineering. His research interests include millimeter-wave power-combining oscillators and amplifiers, quasi-optical techniques, and nonlinear analysis of microwave circuits.

Dr. Mortazawi served as the Orlando IEEE AP/MTT chapter chairman from 1994 to 1995.

Bernard C. DeLoach, Jr. (M'57–F'72–LF'95) received the B. S. and M.S. degrees in physics from Auburn State University, Auburn, AL, in 1951 and 1952, respectively, and the Ph.D. degree in physics from Ohio State University, Columbus, in 1956.

In 1956, he joined Bell Laboratories, as a member of the Radio Research Department. In 1990, he became a Courtesy Professor of engineering science at the University of Central Florida, Orlando. He has worked in the areas of microwave filters, microwave parametric amplifiers, microwave and millimeter-wave solid-state oscillators, light-emitting diodes, semiconductor lasers, and avalanche photo detectors.

Dr. DeLoach received the IEEE's David Sarnoff Award, and the Franklin Institute's Stuart Ballantine Medal, both in 1975, and the IEEE Medal for Engineering Excellence, in 1993. He has served in many areas of IEEE activities.